

# $D \rightarrow \pi, l\nu$ Semileptonic Decays, $|V_{cd}|$ and $2^{nd}$ Row Unitarity from Lattice QCD

Heechang Na,<sup>1</sup> Christine T. H. Davies,<sup>2</sup> Eduardo Follana,<sup>3</sup> Jonna Koponen,<sup>2</sup> G.Peter Lepage,<sup>4</sup> and Junko Shigemitsu<sup>1</sup>  
(HPQCD Collaboration)

<sup>1</sup>*Department of Physics, The Ohio State University, Columbus, OH 43210, USA*

<sup>2</sup>*SUPA, School of Physics & Astronomy, University of Glasgow, Glasgow, G12 8QQ, UK*

<sup>3</sup>*Departamento de Física Teórica, Universidad de Zaragoza, E-50009 Zaragoza, Spain*

<sup>4</sup>*Laboratory of Elementary Particle Physics, Cornell University, Ithaca, NY 14853, USA*

We present a new calculation of the  $D \rightarrow \pi, l\nu$  semileptonic form factor  $f_+^{D \rightarrow \pi}(q^2)$  at  $q^2 = 0$  based on HISQ charm and light valence quarks on MILC  $N_f = 2 + 1$  lattices. Using methods developed recently for HPQCD's study of  $D \rightarrow K, l\nu$  decays, we find  $f_+^{D \rightarrow \pi}(0) = 0.666(29)$ . This signifies a better than factor of two improvement in errors for this quantity compared to previous calculations. Combining the new result with CLEO-c branching fraction data, we extract the CKM matrix element  $|V_{cd}| = 0.225(6)_{exp.}(10)_{lat.}$ , where the first error comes from experiment and the second from theory. With a total error of  $\sim 5.3\%$  the accuracy of direct determination of  $|V_{cd}|$  from  $D$  semileptonic decays has become comparable to (and in good agreement with) that from neutrino scattering. We also check for second row unitarity using this new  $|V_{cd}|$ , HPQCD's earlier  $|V_{cs}|$  and  $|V_{cb}|$  from the Fermilab Lattice & MILC collaborations. We find  $|V_{cd}|^2 + |V_{cs}|^2 + |V_{cb}|^2 = 0.976(50)$ , improving on the current PDG2010 value.

PACS numbers: 12.38.Gc, 13.20.Fc

## I. INTRODUCTION

The Cabibbo-Kobayashi-Maskawa (CKM) matrix provides particle physicists with a wealth of opportunities to carry out precision tests of the Standard Model (SM) and look for New Physics. On the one hand each matrix element can be determined in several ways, employing different experimental and theory inputs, and the results compared with each other. Three generation unitarity can also be examined to see how well  $\hat{V}_{CKM} \times \hat{V}_{CKM}^\dagger = \hat{I}$  is satisfied. This leads to tests such as  $1^{st}$ ,  $2^{nd}$  or  $3^{rd}$  row/column unitarity. It also gives rise to the important “Unitarity Triangle” relation  $V_{ud}^* V_{ub} + V_{cd}^* V_{cb} + V_{td}^* V_{tb} = 0$ . Consistency checks of the sides and angles of the Unitarity Triangle (UT) have been the focus of much of the experimental and theoretical effort in Flavor Physics in recent years. Lattice QCD is playing an increasingly important role in CKM physics [1]. For instance, lattice calculations of the Kaon semileptonic form factor  $f_+^{K \rightarrow \pi}(0)$  [2, 3] and the decay constant  $f_K$  (or  $f_K/f_\pi$ ) [4–8] have contributed to precision determinations of  $|V_{us}|$  and  $1^{st}$  row unitarity tests [9].

The HPQCD collaboration recently published a new lattice calculation of the  $D \rightarrow K, l\nu$  semileptonic decay form factor  $f_+^{D \rightarrow K}(q^2)$  at  $q^2 = 0$  [10] which significantly reduced the error on this quantity compared to previous theory results. This led to a very precise determination of the CKM matrix element  $|V_{cs}|$ . Features in the HPQCD work that made this improvement possible include the use of a relativistic quark action, the “Highly Improved Staggered Quark” (HISQ) action [11], to simulate both light and charm quarks, better data analysis tools and a new method for carrying out chiral/continuum extrapolations. Capitalizing on these developments, we turn here in this article to  $D \rightarrow \pi, l\nu$  semileptonic decays. We

focus on extracting the CKM matrix element  $|V_{cd}|$  by combining theory results for  $f_+^{D \rightarrow \pi}(0)$  with experimental input from CLEO-c [12]. The first unquenched lattice studies of  $D$  semileptonic decays were carried out several years ago by the Fermilab Lattice & MILC collaborations [13]. In that work lattice gauge theory was able to predict the shape of  $f_+(q^2)$  prior to subsequent confirmation by experiment. The theory errors for  $f_+^{D \rightarrow \pi}(0)$  in [13] were  $\sim 10\%$ , and this has remained the dominant error in determinations of  $|V_{cd}|$  from  $D$  semileptonic decays. More accurate determinations have come from neutrino scattering experiments so that the current PDG2010 [14] quotes  $|V_{cd}|$  from neutrino charm production with an error of about  $\sim 5\%$ . With the new lattice calculations described in this article, the accuracy of  $|V_{cd}|$  from  $D$  semileptonic decays is approaching that from neutrino scattering and this provides an important consistency check. We find,

$$|V_{cd}| = 0.225(6)_{exp.}(10)_{lat.}, \quad (1)$$

where the first error is from experiment [12] and the second is the theory error from the Lattice QCD calculation presented here. Eq.(1) is in excellent agreement with the PDG value based on neutrino scattering of  $|V_{cd}| = 0.230(11)$ .

In the rest of this article we describe how the result of eq.(1) was obtained. We work with HISQ valence charm and light quarks on the MILC AsqTad  $N_f = 2 + 1$  coarse ( $a \sim 0.12\text{fm}$ ) and fine ( $a \sim 0.09\text{fm}$ ) lattices. Table I lists the five MILC [15] ensembles employed in this work and some simulation parameters. Compared to [10] we have doubled the statistics on ensembles C1, C2 and F1. The valence charm and light bare quark masses are the same as in [10] with the former tuned to the  $\eta_c$  mass and the latter chosen such that the ratio of  $m_{light}$  to the physical strange quark mass is approximately the same for

TABLE I: The MILC  $N_f = 2 + 1$  ensembles used in the  $D \rightarrow \pi$  semileptonic project. The fourth column gives the valence HISQ light and charm quark masses in lattice units.  $N_{conf}$  is the number of configurations and  $N_{tsrc}$  the number of time sources used for each configuration.

Set	$r_1/a$	$m_l(sea)/m_s(sea)$	$am_{valence}$	$N_{conf}$	$N_{tsrc}$	$L^3 \times N_t$
C1	2.647	0.005/0.050	0.0070	1200	2	$24^3 \times 64$
			0.6207	1200	2	
C2	2.618	0.010/0.050	0.0123	1200	2	$20^3 \times 64$
			0.6300	1200	2	
C3	2.644	0.020/0.050	0.0246	600	2	$20^3 \times 64$
			0.6235	600	2	
F1	3.699	0.0062/0.031	0.00674	1200	4	$28^3 \times 96$
			0.4130	1200	4	
F2	3.712	0.0124/0.031	0.0135	600	4	$28^3 \times 96$
			0.4120	600	4	

valence and sea quarks. In the next section we summarize the formulas for hadronic matrix elements necessary to extract  $f_+^{D \rightarrow \pi}(0)$  and explain how they are related to three- and two-point correlators evaluated numerically on the lattice. These relations are the same as those described in reference [10] so we will be brief. In section III we describe our data analysis and fitting procedures. We employ Bayesian fitting methods and carry out multi-exponential fits to several three-point and two-point correlators at the same time. Section IV discusses chiral and continuum extrapolations of lattice results to the physical limit. We apply the modified z-expansion method developed for  $D \rightarrow K$  semileptonic form factors in [10]. Section V presents our results for  $f_+^{D \rightarrow \pi}(0)$  and  $|V_{cd}|$  and comparisons with other determinations of these quantities. Section VI gives a brief summary and we also include a  $2^{nd}$  row unitarity test with all theory inputs coming from Lattice QCD.

## II. RELEVANT MATRIX ELEMENTS

The most efficient way to calculate  $f_+(q^2)$  at  $q^2 = 0$  is to focus on the scalar form factor  $f_0(q^2)$  and use the kinematic identity  $f_+(0) = f_0(0)$ . The scalar form factor can be determined from the matrix element of the scalar current  $S = \bar{\Psi}_q \Psi_c$  between the  $D$  meson and pion states.

$$f_0^{D \rightarrow \pi}(q^2) = \frac{(m_{0c} - m_{0l}) \langle \pi | S | D \rangle}{M_D^2 - M_\pi^2}. \quad (2)$$

The combination in the numerator of eq.(2) does not get renormalized. The use of absolutely normalized currents is one of the reasons why we are able to significantly reduce errors in our  $D$  semileptonic scalar form factor calculations, both here and in [10].

Our goal is to determine the hadronic matrix element  $\langle \pi | S | D \rangle$  in eq.(2) via numerical simulations. The starting point is the three-point correlator,

$$C^{3pnt}(t_0, t, T, \vec{p}_\pi) = \frac{1}{L^3} \sum_{\vec{x}} \sum_{\vec{y}} \sum_{\vec{z}} e^{i\vec{p}_\pi \cdot (\vec{z} - \vec{x})} \langle \Phi_\pi(\vec{x}, t_0) \tilde{S}(\vec{z}, t) \Phi_D^\dagger(\vec{y}, t_0 - T) \rangle. \quad (3)$$

In eq.(3) the interpolating operator  $\Phi_D^\dagger$  creates a  $D$  meson at time slice  $t_0 - T$ . At time  $t$  ( $t_0 \geq t \geq t_0 - T$ ) the scalar current  $S$  converts the  $c$  quark inside the  $D$  into a light quark and also inserts momentum  $\vec{p}_\pi$ . The resulting pion then propagates to time slice  $t_0$  where it is annihilated by  $\Phi_\pi$ . In addition to the three-point correlator one needs the pion and  $D$  meson two-point correlators,

$$C_D^{2pnt}(t, t_0) = \frac{1}{L^3} \sum_{\vec{x}} \sum_{\vec{y}} \langle \Phi_D(\vec{y}, t) \Phi_D^\dagger(\vec{x}, t_0) \rangle, \quad (4)$$

and

$$C_\pi^{2pnt}(t, t_0; \vec{p}_\pi) = \frac{1}{L^3} \sum_{\vec{x}} \sum_{\vec{y}} e^{i\vec{p}_\pi \cdot (\vec{x} - \vec{y})} \langle \Phi_\pi(\vec{y}, t) \Phi_\pi^\dagger(\vec{x}, t_0) \rangle. \quad (5)$$

Details on how the above three- and two-point correlators can be expressed in terms of single component staggered quark propagators are given in section IV of reference [10] and will not be repeated here. There we also show how the sums  $\sum_{\vec{x}}$  in eqns.(3), (4) and (5) can be carried out using U(1) random wall sources.

The meson creation operators  $\Phi_D^\dagger$  and  $\Phi_\pi^\dagger$  create not only the ground state  $D$  and pion we are interested in but also an arbitrary number of excited states with the same quantum numbers. Hence the  $t$  dependence of the two- and three-point correlators is complicated especially for staggered quarks. For two-point correlators it is given by,

$$C_D^{2pnt}(t) = \sum_{j=0}^{N_D-1} b_j^D (e^{-E_j^D t} + e^{-E_j^D (N_t-t)}) + \sum_{k=0}^{N'_D-1} d_k^D (-1)^t (e^{-E_k'^D t} + e^{-E_k'^D (N_t-t)}), \quad (6)$$

and similarly for  $C_\pi^{2pnt}(t)$ , except that there is no opposite parity terms for zero momentum. For three-point correlators one has

$$C^{3pnt}(t, T) = \sum_{j=0}^{N_\pi-1} \sum_{k=0}^{N_D-1} A_{jk} e^{-E_j^\pi t} e^{-E_k^D (T-t)} + \sum_{j=0}^{N_\pi-1} \sum_{k=0}^{N'_D-1} B_{jk} e^{-E_j^\pi t} e^{-E_k'^D (T-t)} (-1)^{(T-t)}$$

$$\begin{aligned}
& + \sum_{j=0}^{N'_\pi-1} \sum_{k=0}^{N_D-1} C_{jk} e^{-E'_j t} e^{-E_k^D (T-t)} (-1)^t \\
& + \sum_{j=0}^{N'_\pi-1} \sum_{k=0}^{N'_D-1} D_{jk} e^{-E'_j t} e^{-E_k^D (T-t)} (-1)^t (-1)^{(T-t)}.
\end{aligned} \tag{7}$$

We are interested in the ground state contributions with amplitudes,

$$b_0^D \equiv \frac{|\langle \Phi_D | D \rangle|^2}{2M_D a^3}, \tag{8}$$

$$b_0^\pi \equiv \frac{|\langle \Phi_\pi | \pi \rangle|^2}{2E_\pi a^3}, \tag{9}$$

and

$$A_{00} \equiv \frac{\langle \Phi_\pi | \pi \rangle \langle \pi | S | D \rangle \langle D | \Phi_D \rangle}{(2E_\pi a^3) (2M_D a^3)} a^3. \tag{10}$$

So the hadronic matrix element  $\langle \pi | S | D \rangle$  that enters into the formula for  $f_0^{D \rightarrow \pi}(0)$  in (2) is given by,

$$\langle \pi | S | D \rangle = 2\sqrt{M_D E_\pi} \frac{A_{00}}{\sqrt{b_0^\pi b_0^D}}. \tag{11}$$

We have accumulated simulation data for zero momentum  $D$  correlators and for pion correlators with momenta  $\frac{2\pi}{L}(0,0,0)$ ,  $\frac{2\pi}{L}(1,0,0)$ ,  $\frac{2\pi}{L}(1,1,0)$  and  $\frac{2\pi}{L}(1,1,1)$ . The corresponding three-point correlators were calculated for  $T = 15, 16$  on the coarse and for  $T = 19, 20, 23$  on the fine ensembles. In the next section we describe how the combination on the right-hand-side of (11) is obtained from three- and two-point correlators.

### III. FITS AND DATA ANALYSIS

Extracting energies and amplitudes from numerical data on two- and three-point correlators is one of the more challenging but at the same time very important aspect of lattice calculations. For the past decade the HPQCD collaboration has been employing fitting methods based on Bayesian statistics and involving multi-exponential fits [16]. For instance, in order to obtain the ground state energy and amplitude from a two-point correlator, we drop the first  $1 \sim 4$  time slices and then fit to the form of eq.(6) for several values of  $N \equiv N_D$  (or  $N_\pi$ ) and  $N'$ . One continues to increase the number of exponentials until the fit results for  $E_0$  and  $b_0$  including their errors and the chisquared per degree of freedom of the fit have stabilized. Fig.1 shows an example of  $aE_\pi$  versus  $N_{exp} = N_\pi$  for momentum  $\frac{2\pi}{L}(1,1,1)$  with  $N'_\pi = N_\pi$ . One sees that fits have stabilized after  $N_{exp} = 3$ . It should be noted that as one increases the number of exponentials and with it the number of fit parameters, the

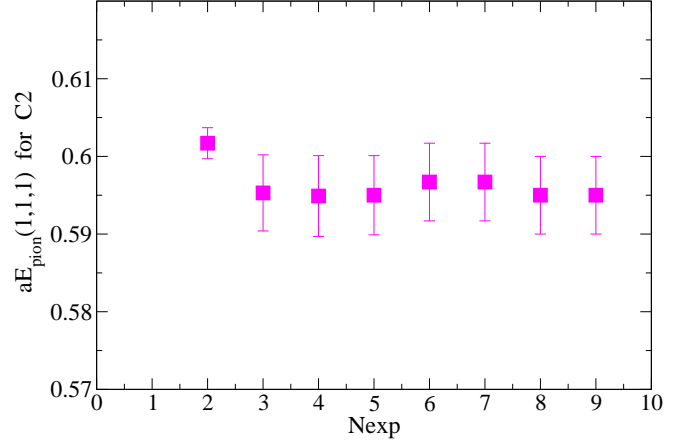


FIG. 1: Ground state pion energy in lattice units for momentum  $\frac{2\pi}{L}(1,1,1)$  versus the number of exponentials in the fit.

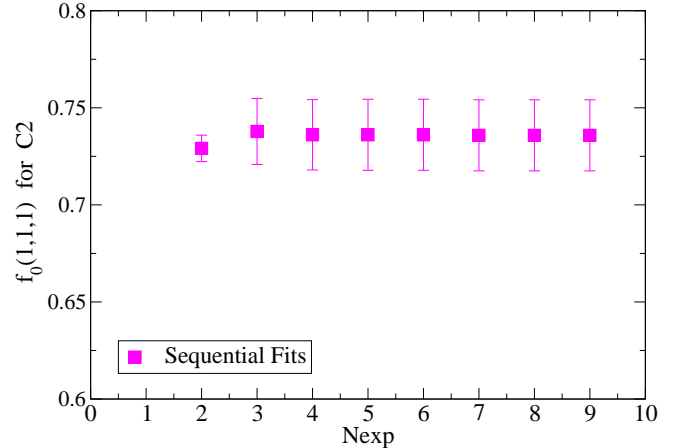


FIG. 2: The form factor  $f_0(q^2)$  for pion momentum  $\frac{2\pi}{L}(1,1,1)$  from simultaneous fits to two- and three-point correlators versus  $N_{exp} = N_D = N'_D = N_\pi = N'_\pi$ . The “sequential fitting” method was employed to go from one  $N_{exp}$  value to the next. In this method the fit results from the  $N_{exp}$  exponential fit is inserted as initial conditions for the subsequent  $[N_{exp} + 1]$  exponential fit.

number of data points is growing as well. Each new fit parameter adds another prior term, i.e. additional data, to the fit function and the number of data points minus the number of fit parameters remains constant [16].

The combination  $\frac{A_{00}}{\sqrt{b_0^\pi b_0^D}}$  is obtained from simultaneous fits to  $C_D^{2pnt}(t)$ ,  $C_\pi^{2pnt}(t)$  and  $C^{3pnt}(t, T)$  for 2 (or 3)  $T$  values. In order to be able to include a large number

of exponentials in these complicated fits we proceed as follows. We set  $N_\pi = N'_\pi = N_D = N'_D \equiv N_{exp}$  and start out with a small value,  $N_{exp} = 2$  or  $N_{exp} = 3$ . The fit results are then inserted as initial conditions for the subsequent  $N_{exp} + 1$  exponential fit. This procedure is repeated until one has completed multi-exponential fits with  $N_{exp}$  much larger than 2. Fig. 2 shows results for  $f_0(q^2)$  on ensemble C2 at pion momentum  $\frac{2\pi}{L}(1, 1, 1)$  versus  $N_{exp}$  using this “sequential fitting” procedure. One sees that, similar to in Fig.1, fit results have stabilized for  $N_{exp} > 3$  [17].

In ongoing work we are investigating further methods to deal with complicated fits with large number of parameters, in particular fits to collections of sums of exponentials [18]. For the calculations of this article, however, we have found that the “sequential fitting” method described above works well for all our data [19]. We are even able to fit data on a given ensemble for all four pion momenta simultaneously and this allows us to obtain correlations between form factor results at different  $q^2$ . These simultaneous fit results for  $f_0(\vec{p}_\pi)$  are given in Table II for several pion momenta  $\vec{p}_\pi$  (the latter in units of  $\frac{2\pi}{L}$ ).

#### IV. CHIRAL AND CONTINUUM EXTRAPOLATION

The next step is to extrapolate the data of Table II to the chiral/continuum limit. We do so using the “modified z-expansion fit” developed in [10]. The scalar form factor is parameterized as

$$f_0(q^2) = \frac{1}{P(q^2)\Phi_0} (a_0 D_0 + a_1 D_1 z + a_2 D_2 z^2) \times (1 + b_1(aE_\pi)^2 + b_2(aE_\pi)^4), \quad (12)$$

with

$$D_i = 1 + c_1^i x_l + c_2^i x_l \log(x_l) + d_i (am_c)^2 + e_i (am_c)^4 + f_i \left( \frac{1}{2} \delta M_\pi^2 + \delta M_K^2 \right), \quad (13)$$

$$x_l = \frac{M_\pi^2}{(4\pi f_\pi)^2}, \quad (14)$$

$$\delta M_\pi^2 = \frac{1}{(4\pi f_\pi)^2} ((M_\pi^{sea})^2 - (M_\pi^{valence})^2), \quad (15)$$

$$\delta M_K^2 = \frac{1}{(4\pi f_\pi)^2} ((M_K^{sea})^2 - (M_K^{valence})^2). \quad (16)$$

The kinematic variable  $z$  is defined as [20–22],

$$z(q^2, t_0) = \frac{\sqrt{t_+ - q^2} - \sqrt{t_+ - t_0}}{\sqrt{t_+ - q^2} + \sqrt{t_+ - t_0}}, \quad (17)$$

TABLE II: Results for  $f_0(\vec{p}_\pi)$  for each ensemble

Set	$f_0(0, 0, 0)$	$f_0(1, 0, 0)$	$f_0(1, 1, 0)$	$f_0(1, 1, 1)$
C1	1.1557(74)	0.9155(93)	0.8119(68)	0.7384(209)
C2	1.1014(38)	0.8700(59)	0.7801(43)	0.7315(87)
C3	1.0398(28)	0.8787(36)	0.7922(31)	0.7326(66)
F1	1.1053(29)	0.8652(52)	0.7586(53)	0.7112(108)
F2	1.0443(28)	0.8613(31)	0.7645(53)	0.7097(70)

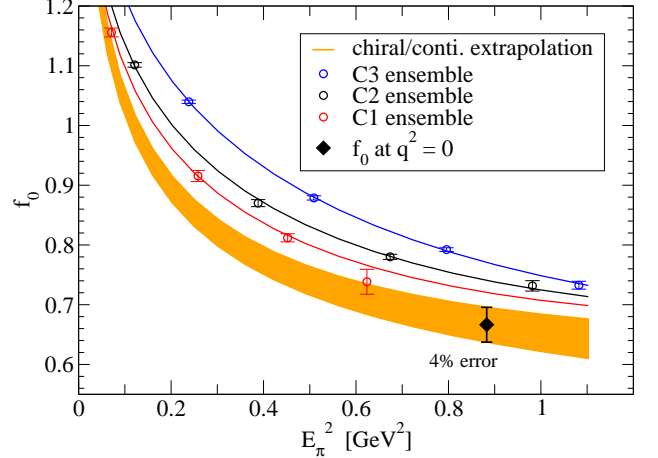


FIG. 3: Chiral/continuum extrapolation of  $f_0^{D \rightarrow \pi}$  versus  $E_\pi^2$ . The data points are from the coarse ensembles (C1, C2 and C3). The three individual curves and the extrapolated band are from a fit to all five ensembles.

with  $t_0$  a free parameter (which we set equal to  $1.95 \text{ GeV}^2$ ) and  $t_\pm = (M_D \pm M_\pi)^2$ . We take  $\Phi_0$  from [21] and set  $P(q^2) = 1$ , where the latter relation reflects the absence of subthreshold poles in the scalar channel.

We show results of fits to the form of eq.(12) in Figs.3 & 4. We plot separately the coarse and fine data points in order to be able to better distinguish individual curves. However, the fit was done simultaneously to all the data in Table II, coarse and fine. The  $\chi^2/dof = 0.85$  for this fit. In Fig.5 we show both  $f_0^{D \rightarrow K}(q^2)$  (results from [10]) and  $f_0^{D \rightarrow \pi}(q^2)$  versus  $q^2$  in the physical region  $0 \leq q^2 \leq q_{max}^2 = (M_D - M_{\pi(K)})^2$ . Note that we consider the correlations between the momenta in the fits which we did not consider in [10]. However, we find that including or excluding correlations in our chiral/continuum extrapolations has minimal effect on  $f_0^{D \rightarrow \pi}(0)$  at the physical point, namely a  $\sim 0.04\sigma$  shift in the central value and a  $\sim 0.02\sigma$  change in the error.

The motivation for the “modified z-expansion fit” is explained in more detail in [10]. Form factors at  $q^2 = 0$  are needed to extract the CKM matrix elements  $|V_{cd}|$  or  $|V_{cs}|$ . The pion energy approaches 1 GeV in this kinematic re-

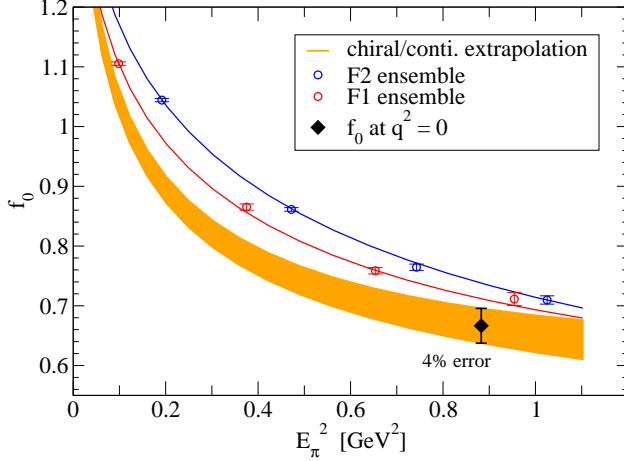


FIG. 4: Same as for Fig.3 showing, however, the fine data points.

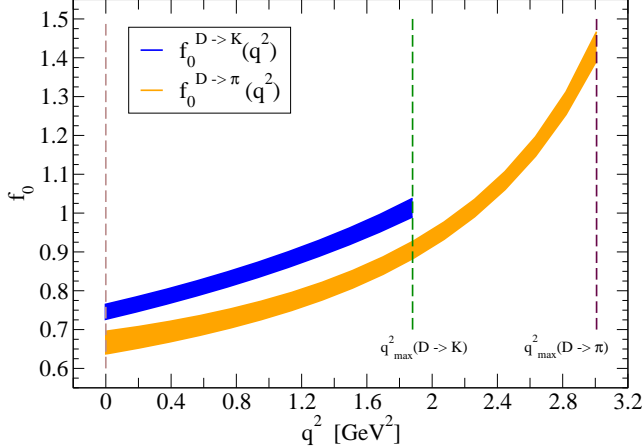


FIG. 5:  $f_0^{D \rightarrow K}(q^2)$  and  $f_0^{D \rightarrow \pi}(q^2)$  versus  $q^2$  in the physical limit.

gion and so chiral perturbation theory might cease to be valid. The z-expansion, on the other hand, is applicable throughout the physical kinematic region, and our new “modified z-expansion” allows for the expansion coefficients to be mass and lattice spacing dependent. We have checked that fits to eq.(12) are stable with respect to adding further terms such as  $x_l^2$ ,  $(am_c)^6$ ,  $(aE_\pi)^6$  or keeping just the  $c_1^i$  and  $c_2^i$  terms in eq.(13) (the  $D_i$ ’s). Such changes in the fit ansatz led to minimal changes in both the central value and the error for  $f_0(0)$  in the physical limit. We have also verified that traditional ChPT extrapolations (see Appendix C & D of [10] and references therein for relevant ChPT formulas) lead to  $f_+(0)$  in the

TABLE III: Error Budget for  $f_+^{D \rightarrow \pi}(0)$

Type	Error (%)
Statistical	3.1
Scale ( $r_1$ and $r_1/a$ )	0.7
Expansion coeff. $a_i$	0.3
$E_p$	0.6
Light quark dependence	1.9
Sea quark dependence	0.6
$am_c$ corrections	2.0
$aE_\pi$ corrections	1.0
Finite volume	0.04
Charm mass tuning	0.05
Total	4.4%

physical limit consistent with the z-expansion result and with comparable errors, however with worse  $\chi^2/dof$ .

## V. RESULTS FOR $f_+^{D \rightarrow \pi}(0)$ AND $|V_{cd}|$ IN THE PHYSICAL LIMIT

Our final result for the  $D \rightarrow \pi$  form factor at  $q^2 = 0$  averaged over  $D^0 \rightarrow \pi^-$  and  $D^+ \rightarrow \pi^0$ , is,

$$f_+^{D \rightarrow \pi}(0) = 0.666(20)_{stat.}(21)_{sys.}, \quad (18)$$

where the first error is statistical and the second systematic. Fig.6 plots our new result together with other theory calculations [13, 23, 24] and experimental determinations [12, 25] (the latter use CKM unitarity values for  $|V_{cd}|$  to extract  $f_+^{D \rightarrow \pi}(0)$ ).

The total error in our  $f_+^{D \rightarrow \pi}(0)$  is 4.4%, signifying a better than factor of 2 improvement over previous lattice determinations. The full error budget is given in Table III. The largest error is statistical followed by  $am_c$  and light quark mass dependence errors. All but the last two entries in Table III were obtained using the methods described in reference [26] and Appendix B of [10]. For instance, the “light quark dependence” errors come from the  $c_1^i$  and  $c_2^i$  terms in the fit ansatz eq.(13), the “ $am_c$  corrections” from the  $d_i$  and  $e_i$  terms etc.

Finite volume errors were estimated by calculating a pion tadpole integral both at finite and at infinite volume. The charm mass tuning error is taken to be the same as for  $D \rightarrow K, l\nu$  for which calculations at two values of  $am_c$  were carried out explicitly to estimate this error. Effects from electromagnetism/isospin breaking and charm sea are expected to give negligible contribution to the error budget compared to our other errors (see [10]).

Finally one can combine our result for  $f_+^{D \rightarrow \pi}(0)$  with CLEO-c’s measurement of  $|V_{cd}| \times f_+^{D \rightarrow \pi}(0)$  [12] to extract a precision value for  $|V_{cd}|$  from D semileptonic decays. This leads to the result quoted already in eq.(1), which is shown in Fig.7 together with values from PDG2010.

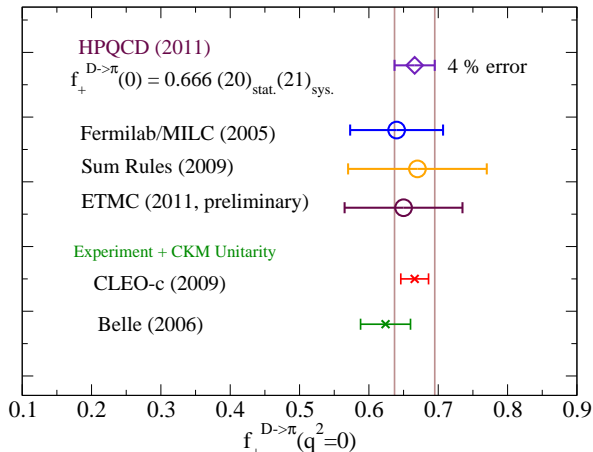


FIG. 6: The  $D \rightarrow \pi$  form factor  $f_+^{D \rightarrow \pi}(0)$  from this work and comparisons with other determinations [12, 13, 23–25].

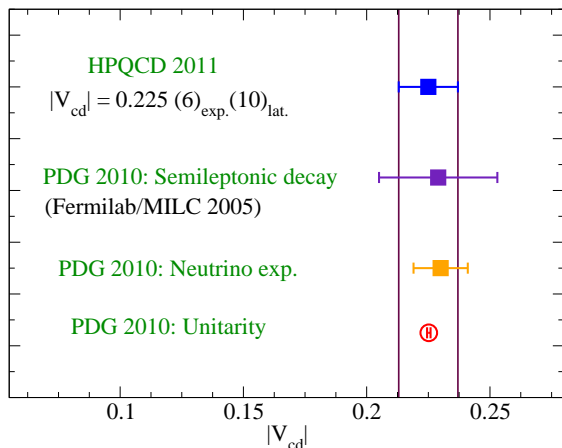


FIG. 7: Comparison of  $|V_{cd}|$  from this work with values in PDG2010 [14].

## VI. SUMMARY

In this article we have presented a new calculation of the  $D \rightarrow \pi, l\nu$  semileptonic form factor  $f_+^{D \rightarrow \pi}(q^2)$  at

$q^2 = 0$ , with errors a factor of two better than in the past. This combined with recent precision measurement of the branching fraction for this process by CLEO-c has allowed for an accurate determination of the CKM matrix element  $|V_{cd}|$ . Direct determination of  $|V_{cd}|$  from  $D$  semileptonic decays is becoming competitive with that from neutrino scattering. The fact that these two very different processes lead to the same  $|V_{cd}|$  is a nontrivial consistency check of the Standard Model.

Finally using our values for  $|V_{cd}|$  and  $|V_{cs}|$  [10] plus the most recent  $|V_{cb}|_{excl.} = 0.0397(10)$  from the Fermilab Lattice & MILC collaborations [27], the most up-to-date test of second row unitarity from Lattice QCD becomes,

$$|V_{cd}|^2 + |V_{cs}|^2 + |V_{cb}|^2 = 0.976(50). \quad (19)$$

This improves on the PDG2010 value  $1.101(74)$  [14].

In the future we will be reducing the largest errors in Table III by increasing statistics and simulating on finer lattices [28]. Calculations of the full  $q^2$  dependence of  $f_+^{D \rightarrow K}(q^2)$  and  $f_+^{D \rightarrow \pi}(q^2)$  are also already underway [28]. Furthermore we are working on updating HPQCD's result for the  $D$  meson decay constant  $f_D$  [5] and on carrying out an independent extraction of  $|V_{cd}|$  from  $D$  leptonic decays [29].

## Acknowledgments:

This work was supported by the DOE and NSF in the US, by STFC in the UK and by MICINN and DGIID-DGA in Spain. We thank MILC for making their Lattices available. Simulations were carried out on facilities of the USQCD collaboration funded by the Office of Science of the DOE and at the Ohio Supercomputer Center.

## Appendix A: Priors and Prior Widths for Two- and Three-Point Correlators

In this appendix we give sample priors and prior widths used in the fits of section III (the reader is referred to reference [16] for definitions of these terms). We turn to the Particle Data Group listings for guidance in picking priors for energies and energy splittings. All energies in Table IV are given in lattice units and are appropriate for ensemble C2. Numbers for other ensembles can be obtained by rescaling with corresponding lattice spacings. Prior widths for amplitudes are fixed based on exploratory initial fits.

[1] For some recent reviews see :  
R. Van de Water, PoS **LAT2009**, 014 (2009);  
V. Lubicz, PoS **LAT2009**, 013 (2009);  
J. Laiho, E. Lunghi and R. Van de Water, Phys. Rev. **D81**, 034503 (2010);  
J. Shigemitsu, [arXiv:1102.0716 [hep-ph]];

J. Laiho, B.D. Pecjak and C. Schwanda, [arXiv:1107.3934 [hep-ex]].  
[2] P. A. Boyle *et al.* [UKQCD/RBC collaboration]; Eur. Phys. J. **C69**, 159-167 (2010).  
[3] V. Lubicz *et al.*, [ETMC], Phys. Rev. D **80**, 111502 (2009)

- [4] A. Bazavov *et al.* [MILC], PoS **LATTICE2010**, 074 (2010).
- [5] E. Follana *et al.*, [HPQCD/UKQCD Collaboration], Phys. Rev. Lett. **100**, 062002 (2008)
- [6] S. Durr *et al.*, [BMW Collaboration], Phys. Rev. D **81**, 054507 (2010)
- [7] Y. Aoki *et al.* [RBC/UKQCD Collaboration], [arXiv:1011.0892 [hep-lat]].
- [8] B. Blossier *et al.* [ETMC], JHEP **0907**, 043 (2009)
- [9] M. Antonelli *et al.*, [FlaviaNet Working Group on Kaon Decays], Eur. Phys. J. C **69**, 399 (2010)
- [10] H. Na *et al.*, [HPQCD collaboration], Phys. Rev. D **82**, 114506 (2010)
- [11] E. Follana *et al.* [HPQCD/UKQCD Collaboration], Phys. Rev. **D75**, 054502 (2007).
- [12] D. Besson *et al.* [CLEO Collaboration], Phys. Rev. D **80**, 032005 (2009)
- [13] C. Aubin *et al.*, [Fermilab Lattice & MILC collaborations], Phys. Rev. Lett. **94**, 011601 (2005).
- [14] K. Nakamura *et al.* [Particle Data Group], J. Phys. G **37**, 075021 (2010).
- [15] C. Bernard *et al.* [MILC], Phys. Rev. **D64**, 054506 (2001).
- [16] G.P. Lepage *et al.* [HPQCD collaboration], Nucl.Phys.B, Proc.Suppl. **106**, 12 (2002).
- [17] For very complicated multi-exponential fits it can happen that fit results include fake low lying levels (with amplitudes that are consistent with zero) that distort ground state energies and fitting errors. Care is required

- to watch out for these spurious levels and make sure that fits that exhibit such levels are not trusted. The “sequential fitting” method adopted in this article has been very effective in preventing spurious levels from arising.
- [18] K. Hornbostel *et al.* [HPQCD collaboration] in preparation.
- [19] In reference [10] the “sequential fitting” method was not employed. Instead the number of exponentials in the three-point correlator ansatz was kept low, at 1 or 2, and only  $N_{exp}$  in the two-point correlators increased as in Figs. 1 & 2. Good  $\chi^2/dof$  were obtained in the simultaneous three- and two-point correlator fits and consistent results for different  $T$  values. We took this as evidence that excited state contributions were suppressed in the three-point correlators compared to in two-point correlators. By simplifying the fit ansatz in this manner, we were able to avoid spurious levels from appearing in [10]
- [20] C.G.Boyd, B.Grinstein and R.F.Lebed; Phys. Rev. Lett. **74**, 4603 (1995).
- [21] M.C.Arnesen *et al.*; Phys. Rev. Lett. **95**:071802 (2005).
- [22] T.Becher and R.J.Hill; Phys.Lett. B**633**, 61 (2006).
- [23] A. Khodjamirian *et al.*, Phys. Rev. D **80**, 114005 (2009).
- [24] S. Di Vita *et al.* [ETMC], [arXiv:1104.0869 [hep-lat]].
- [25] L.Widhalm *et al.* [Belle Collaboration]; Phys. Rev. Lett. **97**:061804 (2006).
- [26] C. T. H. Davies *et al.* [HPQCD Collaboration], Phys. Rev. D **78**, 114507 (2008).
- [27] P. Mackenzie, [Fermilab Lattice & MILC collaborations]; talk presented at CKM2010.
- [28] J. Koponen *et al.* [HPQCD collaboration], work in progress.
- [29] For a recent determination of  $|V_{cd}|$  and  $|V_{cs}|$  from  $D$  leptonic decays see: Y. Namekawa *et al.* [PACS-CS Collaboration]; arXiv:1104.4600 [hep-lat].

TABLE IV: Sample priors and prior widths for two- and three-point correlator fits. Energies are in lattice units, and this example corresponds to priors used for ensemble C2. The notation is the same as in equations (6) and (7).

	prior	prior width
$E_0^D$	1.16	0.58
$E_{j>0}^D - E_{j-1}^D$	0.36	0.36
$E_0'^D$	1.52	1.52
$E_{k>0}'^D - E_{k-1}'^D$	0.36	0.36
$\sqrt{b_j^D}$	0.01	0.5
$\sqrt{d_k^D}$	0.01	0.5
$E_0^\pi(000)$	0.21	0.11
$E_0^\pi(100)$	0.38	0.19
$E_0^\pi(110)$	0.49	0.25
$E_0^\pi(111)$	0.60	0.30
$E_1^\pi(all\ mom) - E_0^\pi(all\ mom)$	0.61	0.31
$E_{j>1}^\pi(all\ mom) - E_{j-1}^\pi(all\ mom)$	0.36	0.36
$E_0'^\pi(100)$	0.74	0.74
$E_0'^\pi(110)$	0.85	0.85
$E_0'^\pi(111)$	0.96	0.96
$E_{k>0}'^\pi(mom > 0) - E_{k-1}'^\pi(mom > 0)$	0.36	0.36
$\sqrt{b_j^\pi(all\ mom)}$	0.01	0.5
$\sqrt{d_k^\pi(mom > 0)}$	0.01	0.5
$A_{jk}, B_{jk}, C_{jk}, D_{jk}$	0.01	0.1